Chapter 14
Nuclear Medicine: An Overview of Imaging Techniques, Clinical Applications and Trials

Amit Mehndiratta, Prabu Anandaraj, Christian M. Zechmann, and Frederik L. Giesel

Abstract Nuclear medicine is a special division of nuclear physics that deals with the application of radioactivity in diagnostic and therapeutic medicine. This chapter will elaborate the basics of nuclear physics, concepts of nuclear imaging radioactive tracers used in nuclear imaging, and their mechanism. Radiation safety is a major concern while administering ionizing radiation for diagnostic or therapeutic purpose. An elaboration on the radiation safety measure for both patient and doctors followed by standardization of nuclear imaging in clinical practice is covered in this chapter. Following this multiple example will be discussed in cancer imaging of brain, lung, breast, GIT, ovary, prostate, etc. This chapter will conclude with future scope for research and outlook for clinical application in nuclear imaging.

Keywords Nuclear medicine • PET • PET/CT • Tumor imaging • Radiotracers

A. Mehndiratta, MBBS, DPhil (Oxon) (✉)
Department of Engineering Science, Institute of Biomedical Engineering,
Old Road Campus Research Building, University of Oxford,
Hedington, Oxfordshire OX3 7DQ, UK
e-mail: dramit.mehndiratta@gmail.com

P. Anandaraj, MBBS, MMST
Advanced Clinical Applications,
GE Healthcare, Chennai, India
e-mail: prarajya@gmail.com

C.M. Zechmann, MD
Department of Diagnostic Radiology and Nuclear Medicine,
Rinecker Proton Therapy Center, Schaeftlarnstr. 133, Munich 81381, Germany
e-mail: christian.zechmann@rptc-1.de

F.L. Giesel, MD, MBA
Department of Nuclear Medicine, University Hospital Heidelberg,
69120 Heidelberg, Germany
e-mail: frederik.giesel@med.uni-heidelberg.de

C.G. Miller et al. (eds.), *Medical Imaging in Clinical Trials*,
DOI 10.1007/978-1-84882-710-3_14, © Springer-Verlag London 2014

Introduction

Nuclear medicine is a fascinating application of nuclear physics. There are about 2,450 known isotopes of the 100 odd elements in the periodic table, out of which only about 300 are natural. The unstable isotopes of an atom attempts to reach the stability by a fission process and by emitting particles and/or energy in the form of radiation. This process is called radioactivity/nuclear decay processes. The unstable isotopes are those having too many protons/neutrons in their atomic nucleus which makes their bond energy unstable and tend to lose energy to the atomic electron or emitted as packet of radiation energy like gamma rays. Such isotope are called radionuclide or radioactive isotope or simply as radioisotope. In this chapter, we will describe the basics of nuclear physics and the various aspects of its application in diagnostic and therapeutic medicine. All aspects will be considered in this chapter, including research and clinical trials.

Basics of Nuclear Physics

The nuclear decay process emits energy in various forms which can be alpha, beta, or gamma radiations. When an unstable atom's nucleus emits two protons and two neutrons in a packet the process is called alpha decay. A proton can release a particle in a process called beta-plus decay, and a neutron can emit a particle in a process called beta-minus decay. Also some energy may emit from the nucleus of unstable atom which results from a process called gamma decay as well as an electron being attracted into the nucleus and being ejected again. Finally there is the rather catastrophic process where the nucleus breaks in smaller units called spontaneous fission.

The final expression is known as the Radioactive Decay Law. It describes the number of radioactive nuclei that will decrease in an exponential fashion with time with the rate of decrease being controlled by the decay constant. Half-life of a radionucleotide expresses the length of time it takes for the radioactivity of a radioisotope to decrease by a factor of two (Table 14.1). Some of the radionucleotides have a relatively short half-life. These tend to be the ones used for medical diagnostic purposes because they do not remain radioactive for very long following administration to a patient and hence result in a relatively low radiation dose. But isotopes with a relatively longer half-life have been used in the past for therapeutic applications in medicine.

Table 14.1 Half-life of radioisotopes

Radioisotope	Half-life (approx.)
^{81m}Kr	13 s
^{99m}Tc	6 h
^{131}I	8 days
^{51}Cr	1 month
^{137}Cs	30 years
^{241}Am	462 years
^{226}Ra	1,620 years
^{238}U	4.51×10^9 years

Nuclear Imaging Technique

The images are obtained by mapping the distribution of an administered radiopharmaceutical within the body. The radiation is emitted from within the patient and subsequently detected in the imaging device, unlike transmitted through the patient from an external X-ray source (CTs and radiographs). The specific organ function depicted is determined by the biological behavior of the radiopharmaceutical. Conventional imaging with the use of a gamma camera is referred to as planar imaging. More recently, the single photon emission computed tomography (SPECT) has been developed which produces axial slice imaging through the body. SPECT uses a gamma camera to record images at a series of angles around the patient, and the resultant data can be processed using filtered back projection and iterative reconstruction algorithms. SPECT gamma cameras can have one, two, or three camera heads. The more advanced imaging is positron emission tomography (PET) that is also an axial projection acquisition-based technique. PET exploits the positron annihilation process where two 0.51 MeV back-to-back gamma rays are produced. If these gamma rays are detected, their origin will lie on a line joining two of the detectors of the ring of detectors which encircles the patient.

It took more than 40 years for the PET to reach its current state as a clinically useful tool. It is primarily due to the challenge in engineering the electronic components of medical imaging instrument to be merged into the contemporary imaging modality. The major breakthrough in positron imaging heralded with the development of positron camera in 1960 which produce planar images [1]. Later the same year, true transaxial positron tomography utilizing a ring system of detectors was produced by Brookhaven National Laboratory group.

With the advent of advanced reconstruction techniques accompanying CT, the PET scanning took a giant leap ahead. The prototype of modern day positron emission computed tomography was first implemented by Phelps and colleagues in the mid-1970s [2].

More recently, the limited anatomical definition of radionuclide imaging has been addressed to some degree by the development of hybrid imaging techniques in which radionuclide imaging devices are combined with computed tomography in a single imaging system [3]. The resulting images display the functional data obtained from the radionuclide distribution (in color), overlaid on the anatomical information from CT (in gray scale) [3]. As the two image data sets are acquired almost simultaneously using the same imaging device, the two data sets can be co-registered very accurately. Not only do these hybrid systems allow abnormalities seen on radionuclide images to be assigned to precise anatomical structures, but they also enable the morphological appearances of disease processes depicted by CT to be assimilated into the interpretation of the findings on radionuclide images. For example, such combined interpretation can aid the distinction of malignant and inflammatory causes of uptake of the positron-emitting radiopharmaceutical ^{18}F-fluorodeoxyglucose (FDG) [4]. Further advantages of hybrid systems include the use of the CT data to correct radionuclide images for artifacts resulting from attenuation of photons travelling through the body and the ability to incorporate radionuclide image data into CT-based radiotherapy planning systems.

Table 14.2 Specific organ where radiopharmaceutical agent or radiotracer accumulates for a short period of time

Body organ	Radiotracer
Brain	^{99m}Tc-ceretec
Thyroid	$Na^{99m}TcO_4$
Lung (ventilation)	^{133}Xe gas
Lung (perfusion)	^{99m}Tc-MAA
Liver	^{99m}Tc-tin colloid
Spleen	^{99m}Tc-damaged red blood cells
Pancreas	^{75}Se-selenomethionine
Kidneys	^{99m}Tc-DMSA

Radiotracer in Human Studies

The radioactivity is generally administered to the patient in the form of a radiopharmaceutical agent or radiotracer. This follows some physiological pathway to accumulate for a short period of time in some specific organ of the body (Table 14.2). A good example is ^{99m}Tc-tin colloid which following intravenous injection accumulates mainly in the liver. The substance emits gamma rays, and we can produce an image of its distribution using a nuclear medicine imaging system. This image can tell us the physiological functional information of the liver or localize the diseased sections.

Nuclear medicine procedures are best served by tracers labeled with a radionuclide that has a physical half-life that is long enough to allow for imaging in a reasonable amount of time, but not so long as to continue to irradiate the patient much beyond that imaging. Thus, radiotracers cannot be stored but must be generated daily for immediate use. To provide for tracers labeled with short-lived radionuclides, generators containing the parent material are constructed to provide an extended source of the daughter; alternatively, the radionuclide may be generated in a medical cyclotron, used to label a tracer, and the tracer shipped to the nuclear medicine department for use. This latter method is generally employed for positron-emitting radionuclides, the exception being rubidium-82, a blood flow PET tracer produced in a generator. The most commonly used radionuclide in nuclear medicine procedures is Tc-99m, and the generation of this radionuclide is from molybdenum-99 (Mo-99)-Tc-99m generator. Discussion on moly-generator is beyond the scope of this book.

Other widely used radionuclide tracers which need to be discussed in detail are the PET radionuclides. The most commonly used radionuclides for PET include fluorine-18 (F-18), carbon-11 (C-11), nitrogen-13 (N-13), and oxygen-15 (O-15). In fact, the successful synthesis of F-18 and the application of 18F-FDG had provided another major drive for the advancement of PET [5, 6].

FDG is the most commonly used tracer for PET but is plagued with false-positivity. For instance, the overall accuracy of FDG-PET in detecting a solitary pulmonary nodule is in the order of 90 %, but false positivity due to granulomatous diseases like tuberculosis leads to incorrect diagnostic categorization due to similar uptake of FDG by affected cells. Tracers that use cellular mechanism for which tumor tissue will be different from that of normal tissue will reduce the incidence of

false positivity. One such mechanism that is prominent for tumor tissue is its high cellular proliferation. Tracer targeting this cellular feature will provide an appropriate diagnostic categorization of tumor tissue. F-18 fluoro-deoxy-L-thymidine (FLT) is a promising candidate which gets incorporated in the DNA in a fashion similar to that of natural thymidine in the cell nucleus. The cellular proliferation is earmarked by mitosis which leads to DNA synthesis and hence specific increased uptake of FLT which can be imaged using FLT-PET. On the downside, organs like the liver and bone marrow have high affinity for FLT even under normal conditions due to high cellular turnover. Hence, FLT is of less use in detecting primary or metastatic lesion in these sites.

Cellular Mechanism of Radiotracers

The success of nuclear medicine applications depends on the detection of signals emitted by an injected radionuclide that is concentrated in the pathological tissue under evaluation. For the radionuclide to concentrate in the specific target tissue, it should be tagged to a modified biomolecule for which the cells at the target location have high affinity for specific uptake. The substitution of radionuclide onto the biomolecules will not significantly alter the reaction time or mechanism of the molecule; hence it is taken up as if it is the natural substrate for the cell.

The common cellular mechanisms that are the targets for tracing the specific uptake of radionuclides are:

1. Glucose utilization of the cell targeting the glycolytic pathway: All cells utilize glucose as a substrate for energy. The glucose is taken up by the cell via GLUT membrane transporter. FDG is a glucose analogue that enters the cells via the same membrane transporters as glucose. Glucose as well as 18F-FDG is phosphorylated by the enzyme hexokinase. In contrast to glucose-6-phosphate, 18F-FDG-6-phosphate is not a substrate for further metabolism in the glycolytic pathway. Therefore, 18F-FDG-6-phosphate is trapped in the cells in proportion to their glycolytic activity [7].
2. Cellular proliferation mechanism: The proliferation rate of a normal cell is different from that of malignant cells. DNA synthesis is high in rapidly proliferating malignant cells. A carefully fluorinated analogue of a pyrimidine or a purine base will behave in the same manner as natural bases and gets incorporated into the DNA of rapidly proliferating tissues. F-18 fluoro-deoxy-L-thymidine (18F-FLT) is a fluorinated analogue of thymidine. The specificity of FLT is high for malignant tumors that have a high cellular proliferation rate relative to that of the nonmalignant tissue. They yield false-positive results for tumors in organs like liver and bone marrow which innately have high cellular turnover.
3. Protein synthesis machinery: Malignant tumors characteristically have high protein synthesis in comparison with benign tumors. Specific amino acids labeled with radionuclide will be taken up by malignant tumors for protein synthesis. A high concentration of radiolabeled amino acid analogues in a

tumor can be imaged using PET scanner. Examples include ^{11}C-methionine and F-18 fluoroethyltyrosine (^{18}F-FET).

4. Choline synthesis: Low-grade tumors have less affinity for ^{18}F-FDG and ^{18}F-FLT. Many low-grade tumors are characterized by high choline content. Presumably these cells are also associated with choline transport and involved in sterol metabolism. ^{18}F-fluorocholine, a radiolabeled choline analogue, has provided promising results in some ^{18}F-FDG false-negative cases [8].
5. Tumor vascularization: Proper vascularization is required for tumor growth and for metastasis. Inadequate vascularization especially in the core of the tumor results in hypoxia and necrosis. Tumor tissue hypoxia could be a good mechanism to target in several solid tumors. ^{18}F-fluoromisonidazole (FMISO) radionuclide tracer is a promising candidate specific for tissue hypoxia in vivo. FMISO in combination with ^{15}O-water perfusion imaging has been used to assess the presence and severity of intratumoral hypoxia, a major determinant of treatment resistance [9]. Another recent addition that targets tissue hypoxia is ^{18}F-fluoroazomycinarabinofuranoside (FAZA) [10].

Radiation Safety

Radiation exposure is a very critical issue which needs to be addressed in all radionuclide studies. If radiation exposure exceeds the permissible limit, it will have effects that may range from trivial to fatal with short-term and long-term sequela-like radiation sickness, vomiting, alopecia, radiation enteritis, GI bleeding, radiation burns, skin carcinoma. On an average, each individual is exposed to a natural background radiation of 3 mSv annually from naturally occurring radioactive materials and cosmic rays from outer space while the largest source of background radiation comes from radon gas. The maximum permissible dose (MPD) per year is for:

- Occupationally exposed individuals—50 mSv:
  - Optimal design goal for restricted area should not exceed 5 mSv/year.
- Individuals who are infrequently exposed or in contact with patients receiving radionuclide therapy—5 mSv.
- General Public—1 mSv.
- Individuals subjected to X-ray security screening—0.25 mSv.

370 MBq of 18F-FDG delivers a dose of 11 mSv to a patient. A patient who has undergone a therapeutic procedure with sealed or unsealed radionuclides may deliver a high radiation dose to people coming in contact with him/her. Hence, a guidance level of 1,000 MBq has been laid as a standard for discharge of patients who had recently undergone radionuclide therapy.

See Table 14.3 for the diagnostic CT effective radiation doses. See Table 14.4 for effective radiation doses for various radionuclide studies.

Table 14.3 Diagnostic CT effective radiation doses

Organ	Radiation dose (mSv)
Head[a,b]	2
Chest[a,c]	8
Abdomen[a,c]	10
Pelvis[a,c]	10

[a]IAEA. Radiation Protection for Patients. Available at: https://rpop.iaea.org/RPOP/RPoP/Content/InformationFor/Patients/patient-information-computed-tomography/
[b]Mettler et al. [107]
[c]Wall and Hart [108]

Table 14.4 Effective radiation dose for various radionuclide studies

Radionuclide study	Radiation dose (mSv)
Lung ventilation (Xe-133)[a]	0.4
Lung perfusion (Tc-99m)[a]	1.2
Kidney (Tc-99m)[a]	2.2–2.5
Thyroid (Tc-99m)[a]	2.6
Bone (Tc-99m)[b]	4.8
Cardiac gated study (Tc-99m)[a]	4.2
PET/CT whole body (F-18 FDG)[c]	7–8

[a]Part 6, Medical Exposure Protection of the Patient. IAEA Training Material on Radiation Protection in Nuclear Medicine. Available at: https://rpop.iaea.org/RPOP/RPoP/Content/Documents/TrainingNuclearMedicine/Lectures/RPNM_Part06_medical_exp_WEB.ppt
[b]IAEA. Radiation Protection for Patients. Available at: https://rpop.iaea.org/RPOP/RPoP/Content/InformationFor/Patients/patient-information-computed-tomography/
[c]IAEA Radiation Protection for Patients (RPOP), PET/CT Scanning. Available at: https://rpop.iaea.org/RPOP/RPoP/Content/InformationFor/HealthProfessionals/6_OtherClinicalSpecialities/PETCTscan.htm

Radiation Exposure to the Workers

The total average exposure for a radiology technician or technologist results in an annual dose equivalent of only 1–1.5 mSv, whereas for the nuclear medicine technologist, it is 2–2.5 mSv. The majority of whole-body radiation to the nuclear medicine worker comes from exposure to the dosed patient during imaging.

Radiation Exposure to the Patient

As most nuclear medicine procedures require an injection of radioactive material attached to a tracer, utmost care must be taken to ensure that the correct procedure has been selected to maximize diagnostic suitability, that the radioactivity of the

injected dose follows the principles of ALARA (as low as reasonably achievable) or ALARP (as low as reasonably practicable), and that the patient has been given adequate information prior to the procedure and such aftercare details as are appropriate. All nuclear medicine procedures require that precautions be taken when administering radioactive materials to females of child-bearing age.

Good Clinical Practice (GCP) and Good Manufacturing Practice (GMP)

Knowledge and compliance with the good clinical practice (GCP) is essential for everyone involved in clinical research trials for nuclear medicine. Clinical trials should be carried out within the framework of a good clinical practice environment in accordance with international guidelines and regulations as detailed in the Declaration of Helsinki [11, 12]. The International Commission of Radiological Protection and the World Health Organization (WHO) have publications that deal with this issue in clinical research. While GCP should form the backbone to successful nuclear medicine clinical studies, radiopharmaceuticals used in these trials need to be produced according to the good manufacturing practice (GMP) [13].

Radiopharmaceuticals for clinical research purposes must be manufactured in accordance with the basic principles of GMP. Due to their short half-lives, many radiopharmaceuticals are administered to patients shortly after their production, so some elements of the quality control may be retrospective. Therefore, strict adherence to GMP is essential. Special attention should be given to the production area environment and personnel, the two basic requirements of GMP production.

Quality Control

Since lots of confounding parameters exist in nuclear medicine, it is a good practice to stick to certain established standards laid by the regulatory bodies, advisory committee, professional organization, and manufacturer's guidelines to ensure quality control of the imaging equipment, radiopharmaceutical tracers, procedure, and imaging protocol. Quality control starts at the time of installation and continues throughout the life cycle of the equipment. It is an ongoing process involving measurements and analyses designed to ensure that the performance of a procedure or instrument is within a predefined acceptable range and to keep it operating at peak performance all the time [14]. Therefore, it is a critical component of routine nuclear medicine practice. A detailed explanation on the quality control program is beyond the scope of this book.

The common quality control measures followed routinely in nuclear medicine practice are:

- Uniformity calibration.
- Spatial linearity.
- Energy resolution and peaking.

- Pixel size calibration.
- Center of rotation correction.
- Tomography resolution.
- Normalization scan.

Uniformity Calibration

The uniformity in the performance of the crystal detector is important for the diagnostic quality of all images. Any nonuniformity in the performance can be demonstrated by an image called the flood image that is irradiated by a uniform distribution of radioactivity. From the high-count flood image of a particular radionuclide, the uniformity (or sensitivity) correction table is derived for that radionuclide which is essentially the pixel-by-pixel ratio of the calculated mean count per pixel to the actual count per pixel in the flood image. Causes of nonuniformity may be due to cracked crystals because of mechanical trauma or temperature excursion beyond threshold, improper tuning of photopeak of radionuclide with the photopeak energy window of camera, uncoupling of photomultiplier tubes from crystals, corrupted software correction tables, etc. Pixel-by-pixel multiplication of an uncorrected image by the ratio image thus calculated gives an image corrected for the nonuniformity.

Uniformity calibration could be evaluated either intrinsically by a point source of ^{99m}Tc placed at about 5 crystal dimensions in the z direction from the center of the uncollimated detector so that a uniform photon flux spreads over the detector (with a count rate of >25,000 cycles/second) or extrinsically by using a sheet source of ^{57}Co placed over the collimated detector (with a count rate of 10–15 million cps). This yields the integral and differential uniformity which expresses the deviation from flood image uniformity.

In current generation nuclear imaging systems, the integrated software solution provides uniformity correction tables that can be easily updated, processed, stored, and automatically applied.

Spatial Resolution

Spatial resolution is the power to discriminate two closely placed point sources distinctly. The overall resolution of a gamma camera is based on the sum of intrinsic spatial resolution of the detector system and the geometric resolution of the collimator. To evaluate the spatial resolution of a gamma camera, a wide variety of test patterns have been developed over the years. The most common test pattern is the four-quadrant bar phantom, which accounts for over 80 % of all resolution patterns used in nuclear medicine. Apart from this, several other test phantoms are available. All these provide a qualitative index of resolution. Correct use of these phantoms requires that all images be compared with a reference image. This reference image can be obtained during acceptance testing or when a quantitative measurement of intrinsic resolution is being performed on the system.

The modulation transfer function (MTF) is an index that exhibits the ability of a gamma camera to yield an image corresponding exactly with the physical distribution of the radionuclide.

Spatial Linearity

Spatial linearity may be affected with nonuniformity due to ill-defined factors like variations in crystal thickness. Spatial linearity correction is done by presenting the camera with an image consisting of a series of parallel straight lines aligned with either the *X* or *Y* axis of the camera. The deviation between the true position of each point on the line, as calculated from a best-fit straight line, and the image of the line, is recorded and stored as a correction factor to be applied to subsequently acquire clinical images.

The correction is generally performed on a weekly basis using either intrinsic or extrinsic techniques.

With this basic idea of nuclear physics, imaging, radiopharmaceuticals, and quality monitoring, we will now proceed to organ-based applications of the technique as a problem-solving tool in medicine.

Nuclear Imaging in Oncology

Positron emission tomography (PET) is an imaging technique based on nuclear physics principles that provides in vivo measurements in absolute units of a radioactive tracer. One of the attractive aspects of PET is that the radioactive tracer can be labeled with short-lived radioisotopes of the natural elements of the biochemical constituents of the body (^{18}F-fluoro-2-deoxy-glucose or [^{18}F]-FDG). This provides PET with a unique ability to detect and quantify physiologic and receptor processes in the body, particularly in cancer cells, which is not possible by any other imaging techniques today. Oncologic PET studies now represent almost 90 % of all clinical studies performed in clinical PET centers worldwide [15–19].

Although ^{18}F-FDG is the most commonly used positron-emitting tracer in PET imaging, there are measurement of tissue blood flow, oxygen metabolism, glucose metabolism, amino acid and protein synthesis and nucleic acid metabolism that have all been demonstrated in PET oncology clinical studies using other tracers [20–23]. Labeling of a large array of other compounds including hypoxic markers, amino acids, DNA proliferation markers, and chemotherapy drugs with ^{11}C and ^{18}F has been studied in various clinical trials (Table 14.5) [17, 22, 23].

The practical and ethical issues associated with PET examination poses difficulty in the conduct of randomized controlled trials; thus, the establishment of diagnostic accuracy and impact on patient management are mainly obtained from clinical practice [18, 24]. There is increasing evidence for the role of PET in staging, monitoring treatment response and biologic characterization of tumors [15–19, 21–23, 25–30].

Table 14.5 Positron-emitting radionuclides used in oncology clinical studies

Radionuclide	Half-life
^{15}O	122 s
^{13}N	9.97 min
^{11}C	20.4 min
^{18}F	109.8 min
^{124}I	4.17 days
^{86}Y	14.7 h
^{64}Cu	12.8 h

Brain Tumor

The evaluation of brain tumors with ^{18}F-FDG PET is a well-established oncologic application of PET. Tumor grade can be assessed accurately and noninvasively by ^{18}F-FDG PET, as the rate of glucose (tracer) utilization is directly proportional to the degree of malignancy [31]. This can be used in the planning of biopsies, and in monitoring high-grade recurrence, particularly in patients with low-grade glioma. Increased ^{18}F-FDG uptake is seen in high-grade glial tumors, as well as in primary cerebral lymphomas, pilocytic astrocytomas, and some unusual tumors (e.g., pleomorphic xanthoastrocytoma, low-grade gliomas). Primary brain tumors (e.g., meningiomas) do not usually show increased ^{18}F-FDG uptake except in more aggressive tumors and in postradiation meningiomas.

Secondary cerebral metastases occur in almost 20–40 % of systemic malignancies and may be the initial presentation of malignancy in 16–35 % of cases. ^{18}F-FDG PET has been extensively studied in these patients with a sensitivity ranging from 68 to 79 % [32]. The principal constraint in using FDG-PET for evaluation of secondary metastasis is the frequent hypometabolic nature of cerebral metastases, and in addition, metastatic lesions are often small (<1 cm in size), and because metastases most often occur at the interface between grey and white matter, identification of lesions can be challenging.

FLT could be used in a limited number of cases suspected of rapidly progressing proliferating brain tumor. C-11 methionine is another radionuclide that is being extensively evaluated for its application in the detection of brain tumor. Unlike FDG, the uptake of ^{11}C-methionine in the human brain is almost negligible. Since the proliferation rate of many brain tumors is relatively low, radiolabeled amino acid analogues are more sensitive than FLT [10]. Currently, the production yield of ^{11}C-labeled radioligand is far below its requirement, thus its practical application is faced with difficulty. F-18 fluoroethyltyrosine (F-18 FET) is a promising alternative fluorinated amino acid analogue whose preliminary studies in brain tumor evaluation appear promising [33].

Lung Carcinoma

There have been numerous studies examining the accuracy of ^{18}F-FDG PET in evaluating solitary pulmonary nodules [34–36]. Analyzing the published data has shown

a high sensitivity of 96 % and accuracy with 94 % in determining this malignancy [16, 23, 37]. Staging in non-small cell lung carcinoma (NSCLC) is very crucial in treatment planning. Studies that have evaluated the role of ^{18}F-FDG PET for staging have reported sensitivity of 82–100 % and specificity of 73–100 % [25, 30, 38–41]. In all series, ^{18}F-FDG PET has been shown to outperform CT in staging lymph node spread in up to 24 % of patients [39]. False-negative results often arise where small lesions are present (<0.6 cm), due to the resolution limitations of PET scanners, respiratory motion over the acquisition period or with certain types of lung cancer such as bronchoalveolar and carcinoid. Figure 14.1a, b shows PET/CT images with DOTATOC tracer from a patient with recurrent lymph node metastases with primary lung cancer. Figure 14.2a, b shows PET/CT image from a patient with pulmonary carcinoid tumor in left lower lobe with metastases to liver. DOTATOC (DOTA(0)-Phe(1)-Tyr(3)-octreotide) is a highly specific PET tracer to somatostatin receptor (SSR2) of neuroendocrine tumor [42, 43].

Colorectal Carcinomas

Primary colorectal cancers occasionally present as an incidental finding on ^{18}F-FDG PET, and ^{18}F-FDG uptake has been reported in adenomatous polyps, a precursor for colon cancer [44]. However, the presence of physiological gut uptake of FDG combined with false-positive uptake in inflammatory disease along with low sensitivity to lesions less than 1 cm precludes a significant role for FDG-PET in primary diagnosis or screening [45]. The role of PET in primary colon cancer remains limited and should be reserved for clinical situations where resection of metastatic disease requires accurate staging of distant spread. PET is an excellent tool in detecting secondary metastasis to liver or extrahepatic abdominal metastases. In published series, the accuracy of ^{18}F-FDG PET in identifying metastatic colorectal carcinoma in the liver has ranged from 90 to 98 % [23] and in extrahepatic diseases, it ranges from 92 to 93 %. In patients with elevated serum CEA markers, occult disease (often extrahepatic recurrence) has been identified accurately with ^{18}F-FDG PET [46].

In advanced rectal cancer, where ^{18}F-FDG PET has been shown to have a significant impact on management in up to one third of patients planned for preoperative adjuvant treatment (chemoradiation), indicating the potential role of ^{18}F-FDG PET in this clinical setting [47].

Lymphoma

The sensitivity and specificity of 18F-FDG PET in detecting the sites of lymphoma has been reported as 86 %–90 % and 93 %–96 % respectively and is considerably superior to CT scans. 18F-FDG PET aids in staging Hodgkin's and non-Hodgkin's lymphoma (NHL) with high acuity. [4, 16, 23]. ^{18}F-FDG PET has been also shown to change the

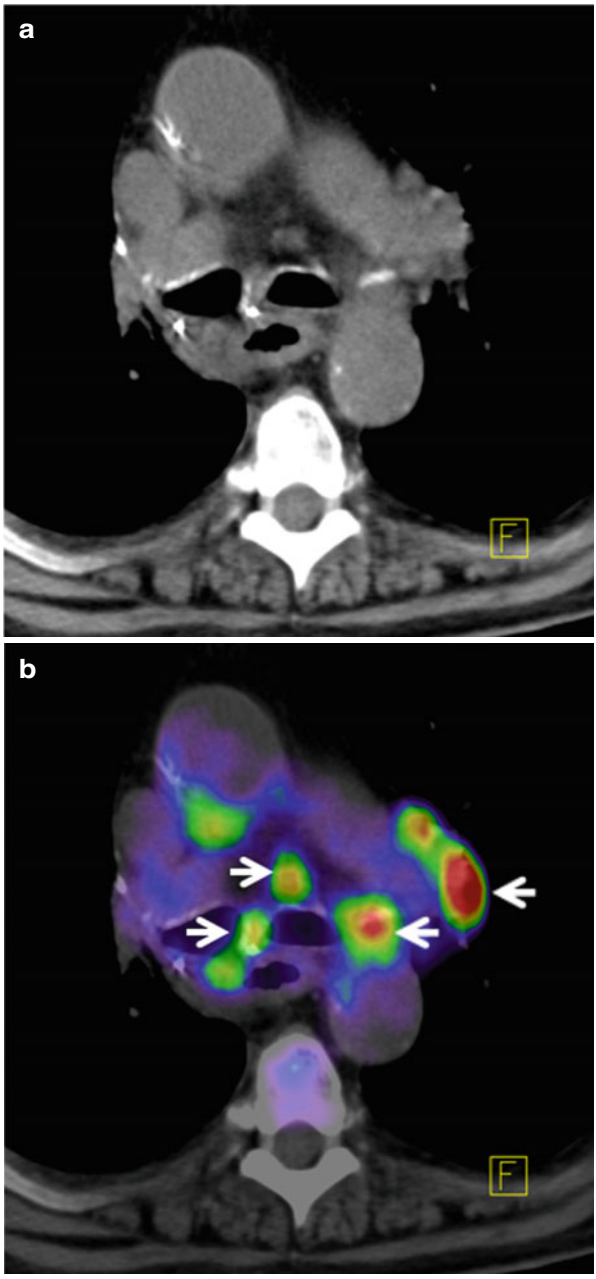

Fig. 14.1 (**a**) Axial slice from CT thorax level of the mediastinum presenting a patient with recurrent lymph node metastases from primary lung cancer. (**b**) Co-registered PET/CT images with high FDG tracer uptake indicating lymph node metastases shown with *arrows*

management in up to 40 % of patients undergoing staging at initial diagnosis [48–51]. In comparison to ^{67}Ga scans, ^{18}F-FDG PET has been shown to have a greater sensitivity for disease detection (particularly spleen) and in view of the potential advantage of a

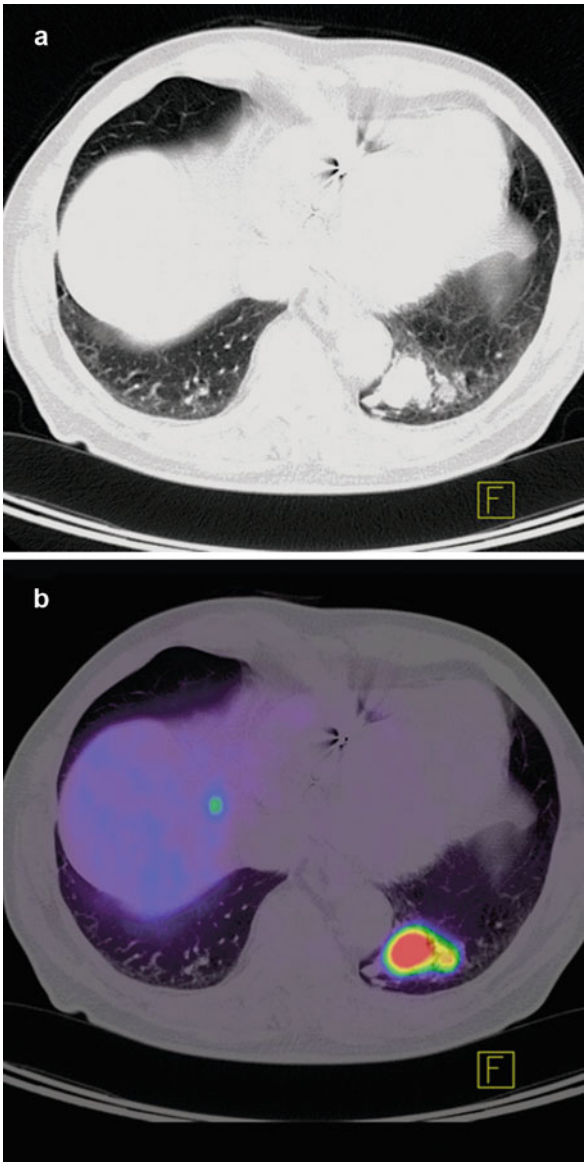

Fig. 14.2 CT (**a**) and PET-CT (**b**) axial slice of chest from a patient with pulmonary carcinoid tumor in the left lower lobe. The neuroendocrine differentiation of the tumor leads to an intense somatostatin receptor (SSR2) overexpression on which the somatostatin analogue 68Ga-DOTATOC tracer can bind. Physiologically SSR2 is expressed only in pituitary, thyroid, adrenals, and excretory organs; any other representation is considered pathological

same-day procedure has supplanted ^{67}Ga scans in many oncology centers [52]. ^{18}F-FDG PET is now routinely performed as part of the assessment of treatment response for NHL; it has also shown to be superior to conventional imaging and to be a strong prognostic indicator of response and progression-free survival [53, 54]. ^{18}F-FDG PET therefore has a major role in both the initial staging and restaging/therapy response assessment of patients with lymphoma. Figure 14.3 shows PET images before, during, and after chemotherapy from patient with Hodgkin's lymphoma.

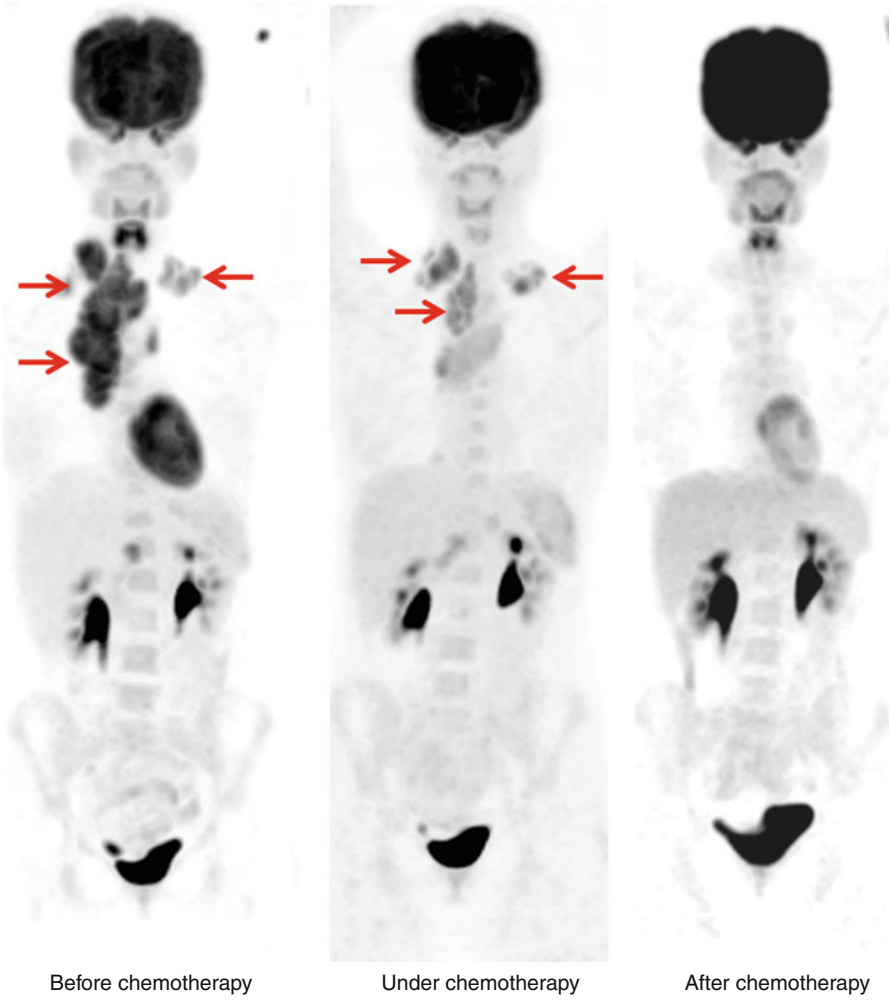

Fig. 14.3 Patient with Hodgkin's lymphoma before (*left panel*), under (*middle panel*), and after several cycles of chemotherapy (*right panel*) showing high FDG uptake of in the cervical and mediastinal region (*arrows*) which decline after several cycle of chemotherapy—metabolic component (FDG-PET) is the leading imaging modality in these tumor entities for tumor response assessment

Melanoma

Malignant melanoma can spread widely and unpredictably throughout the body, and median survival after the appearance of distant metastases is approximately 6 months [55] which makes it very critical to be detected at an early phase. The accuracy of ^{18}F-FDG PET in detecting metastatic melanoma has been reported to range

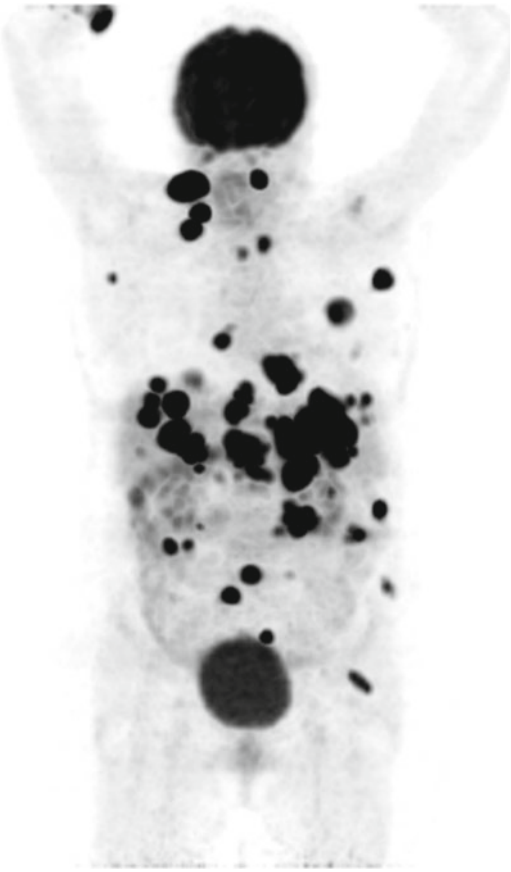

Fig. 14.4 Maximum intensity projection in coronal plane of body presenting FDG PET uptake in a patient with metastasized malignant melanoma

from 81 to 100 %, and in one series of 100 patients demonstrated a sensitivity of 93 % [27]. ^{18}F-FDG PET has been shown to be particularly sensitive in detecting subcutaneous and visceral metastases (Fig. 14.4). In published studies and meta-analyses of the literature, ^{18}F-FDG PET has been demonstrated to detect disease up to 6 months earlier than conventional techniques and alter management in 22–32 % of patients, principally by altering plans for surgical resection of metastatic disease [27, 56, 57]. The role of ^{18}F-FDG PET in melanoma is therefore principally in the evaluation of extent of metastatic disease, the accurate assessment of which can alter patient management particularly where surgery is planned.

Head and Neck Tumors

The presence of lymph node spread of head and neck tumors is associated with substantially worse prognosis which needs to be addressed in early phases. In patients with head and neck tumors studied prior to initial surgery, the sensitivity and

specificity of ^{18}F-FDG PET in detecting nodal metastases has been reported ranging from 71 to 91 % and 88 to 100 %, respectively [23, 58–60]. In patients studied after initial treatment of metastatic nodal disease with radiotherapy, ^{18}F-FDG PET is often accurate only after a 3-month period [35, 61–63]. In both patient groups, the accuracy of PET has the potential to direct surgeons to otherwise unexpected sites of metastatic disease, as well as in avoiding surgery at areas where the scan is negative. ^{18}F-FDG PET has also been shown to be a prognostic factor for radiotherapy response [64].

Breast Carcinoma

In primary breast tumors, ^{18}F-FDG PET has been shown to have a mean sensitivity and specificity for tumor detection of 88 and 79 % respectively in a recent meta-analysis [65]. Axillary nodal involvement is a critical issue in the management of patients with breast carcinoma and ^{18}F-FDG PET has been shown to have a sensitivity ranging from 57 to 100 % and specificity of 66–100 % across reported series [23] in detecting sentinel node involvement. One potential area where ^{18}F-FDG PET has shown great promise is in whole-body staging of metastatic breast cancer, where the accuracy of ^{18}F-FDG PET has been shown to be higher than conventional staging techniques [66, 67]. But certainly FDG-PET is not the best modality of choice for detecting primary carcinoma as most of primary breast tumors are FDG negative.

Gastroesophageal Carcinoma

^{18}F-FDG PET has been shown to significantly improve detection of hematogenous and distant lymphatic metastasis in carcinoma of the esophagus and gastroesophageal junction (GEJ) [34, 68–70]. There is no difference in accuracy in detecting squamous cell carcinoma or adenocarcinoma of the esophagus with ^{18}F-FDG PET. ^{18}F-FDG PET may not be as accurate as USG or CT in determining wall invasion or close lymph node spread of disease; however, the diagnostic specificity of lymph node involvement is greatly improved with PET [70]. ^{18}F-FDG PET is more accurate in detecting distant disease and is also highly accurate in the diagnosis of recurrent disease [68–71].

Ovarian Carcinoma

Ovarian carcinoma is one of the leading causes of death among gynecological malignancies [72]. The treatment of ovarian carcinoma primarily consists of surgical resection followed by chemotherapy or radiotherapy. Accurate staging is very much essential, particularly in the restaging of patients with elevated serum markers (CA-125). ^{18}F-FDG PET has been shown to have high accuracy in detecting in ovarian carcinoma lesions greater than 1 cm in size, but the detection of micrometastatic disease (one of the most

important issues in this disease) has been difficult [73–75]. The role of PET in ovarian carcinoma is very much restricted to post-therapy monitoring of lesion recurrence.

Prostate Cancer

Due to the slow growth and the accompanying low glucose metabolism, sensitivity of FDG-PET is low in diagnosing prostate cancer and metastases thereof (18–65 %; [76, 77]). Also in lymph node metastases smaller than 1 cm, sensitivity and specificity is low [78].

Above all, there is a great overlap of FDG uptake in tumors and benign prostate hyperplasia (BPH, [79]). Furthermore, the high residual activity in the bladder after renal excretion superimposes the uptake in the prostate.

Due to these limitations, other tracers were tested to improve sensitivity. These are ^{11}C- and ^{18}F-labeled cholines. Since cholines are metabolized to membrane phospholipids, the renal excretion is low, and the tracer is accumulated in dividing tumor cells. With choline, a higher sensitivity is possible in detection of metastasized prostate cancer [80]. In BPH the distribution is lower and more homogeneous compared to the tracer uptake in tumors.

^{18}F-fluoromethyl-dimethyl-2-hydroxyethyl-ammonium (FCH) is accumulated in primary tumor, as well as soft tissue and bone metastases [81]. It shows even in smaller lymph nodes a high sensitivity of 66 % and specificity of 96 % [82]. In one study it was shown that ^{11}C-acetate was superior to FDG-PET in detecting recurrent tumor (59 % vs. 17 %, [83]). However, there is an overlap in SUV values of tumor and BPH as well [84]. Figure 14.5a–c shows PET/CT image with FCH tracer from patient with recurrent prostate cancer. Prostrate-specific membrane antigen (PSMA) is a recently introduced small molecule which is specific to prostate cancer cells [85], however uptake by colon cancer and ENT tumors has also been reported. Figure 14.6a–c shows the PET image from one of the patients for whom total prostate resection was performed 3 years ago, now presenting with high PSA serum indicating recurrence of prostate cancer.

L-methyl-^{11}C-methionine is also superior to FDG-PET in lesion detection with a sensitivity of 72.1 % against 48 % for FDG-PET [86]. More than 95 % of metabolically active sites showed metabolism of 11C-methionine; whereas 18F-FDG showed metabolic activity in only 65 % of active sites [86]. However, a significant proportion of lesions (26 %) had no detestable metabolism with either of the two tracers [86].

Nuclear Imaging in Central Nervous System

SPECT and FDG-PET are used to provide complimentary information to the anatomical imaging offered by other conventional modalities (CT/MRI). New methods of imaging neurotransmitter receptors and transporters have been developed and offer expanded roles for brain SPECT. Nuclear medicine can make valuable contributions to the diagnosis and follow-up of patients with dementia, cerebrovascular disease, movement disorders, brain tumors, and other neurological diseases.

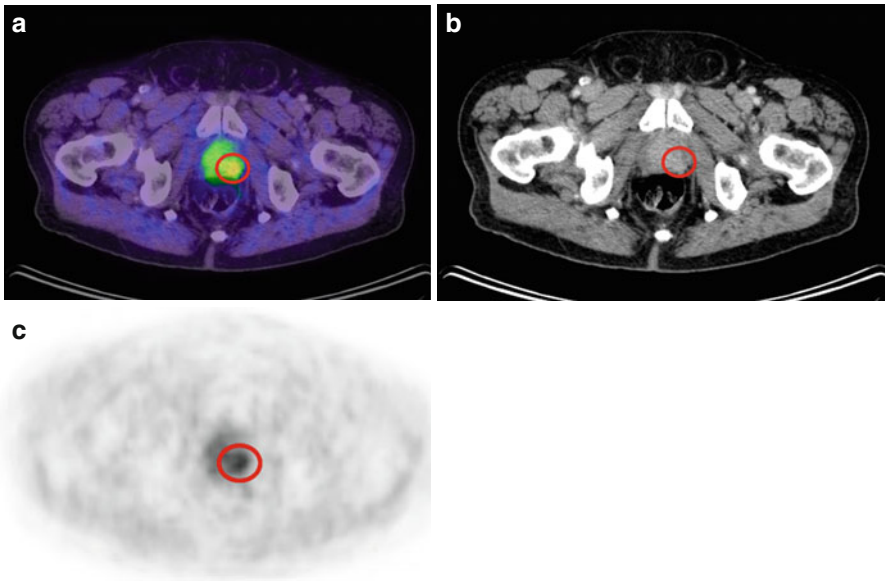

Fig. 14.5 FCh-PET/CT (**a**), CT (**b**), and FCh-PET (**c**) in transverse plane presenting high tracer uptake in a patient with recurrence of prostate cancer (red circle indicating the tumor in the left peripheral zone)

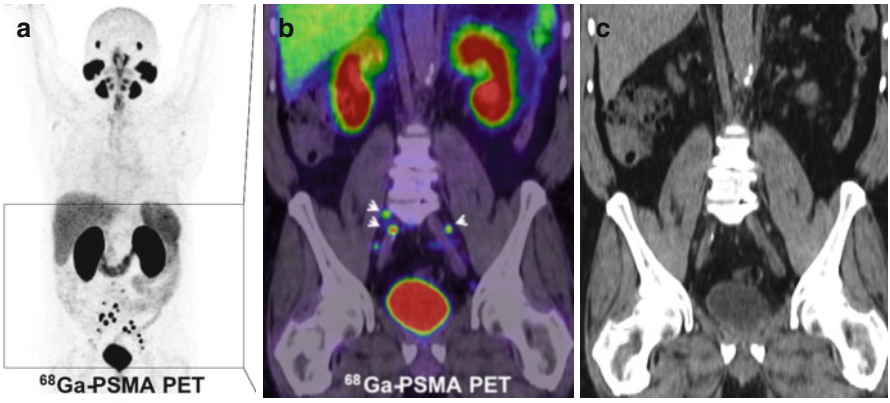

Fig. 14.6 A patient with an elevated PSA serum level as indicator of recurrence of prostate cancer after total prostate resection 3 years ago. Patient was imaged with a recent introduced new small molecule PET tracer called prostate-specific membrane antigen (*PSMA*). (**a**) Presenting whole-body distribution of ^{68}GaPSMA PET in MIP technique. (**b**) PSMA is specific and taken up by prostate cancer cells (presenting strong uptake in these lymph node (*arrow*) in the pelvis region) indicated recurrence of prostate cancer. The coronal CT (**c**) small lymph nodes close to the ilio-psoas muscle on both sides can be appreciated without suspicious enlargements (<1 cm)

The exclusive metabolic substrate of brain is glucose, but the brain has virtually no means of storing energy and is totally dependent on cerebral blood flow for the delivery of glucose and oxygen. Glucose is oxidized to yield ATP, the energy currency of the neurons. The metabolic demand owing to neuronal activity increases the blood flow delivering oxygen and glucose to the particular area of brain, and there exists a close coupling of neuronal activity and blood supply. This feature is exploited in brain activation studies with ^{15}O-H_2O PET, BOLD MRI, and occasionally activation studies with regional cerebral blood flow SPECT (rCBF SPECT).

Conversely, reduced function of parts of the brain will result in a reduction in regional cerebral blood flow, although such hypofunctioning areas may appear anatomically normal on structural imaging with CT or MRI. This ability of rCBF SPECT to reflect brain function is its key strength and it should be regarded as a complementary method of investigation to structural imaging methods.

Dementia

Alzheimer's disease (AD), predominantly a disease of elderly, presents clinically with memory and cognitive impairment. AD is primarily a clinical diagnosis. Pathologically it is characterized by neurofibrillary tangles comprising of abnormal hyperphosphorylated tau protein and extracellular beta amyloid. The classic metabolic abnormality associated with AD is bilateral temporoparietal hypometabolism (Fig. 14.7a, b). The FDG-PET showing hypometabolism of temporoparietal area confirms the diagnosis with 82 % diagnostic accuracy. If FDG-PET scans indicated a metabolic pattern other than bilateral temporoparietal hypometabolism, a cause of dementia other than AD should be suspected [87]. Newer radioligands like AZD2184 labeled with carbon-11 that binds to A beta deposits, associated with the pathogenesis of AD, provide improved contrast when compared with currently used PET radioligands for visualization of A beta deposits [88].

The rCBF SPECT study using the radiopharmaceuticals like hexamethyl propylene amine oxime (HMPAO) and ethylene cysteine dimer (ECD) may show hypometabolism of temporoparietal region in AD with predictive value ranging anywhere from 60 to 96 % [89].

It may not be superior to clinical diagnosis based on detailed neuropsychological testing using NINCDSADRDA (National Institute of Neurological and Communicable Disease and Stroke/Alzheimer's Disease and Related Disorders Association) criteria, but rCBF SPECT has higher specificity and can be used to distinguish dementia due to AD and other causes even without any established CSF biomarkers [90, 91].

Vascular dementia is the second most common dementia after AD caused by ischemic or hemorrhagic cerebrovascular disease (atherosclerosis of large cerebral vessels, hypertension, cerebral amyloid angiopathy, etc.) or by ischemic-hypoxic brain lesions of cardiovascular origin. rCBF SPECT is dependent on the perfusion of cells and is largely a gray matter imaging technique, but vascular dementia may be associated with white matter ischemia without any cortical infarct. Hence, SPECT is of limited use in white matter disease where the uptake of

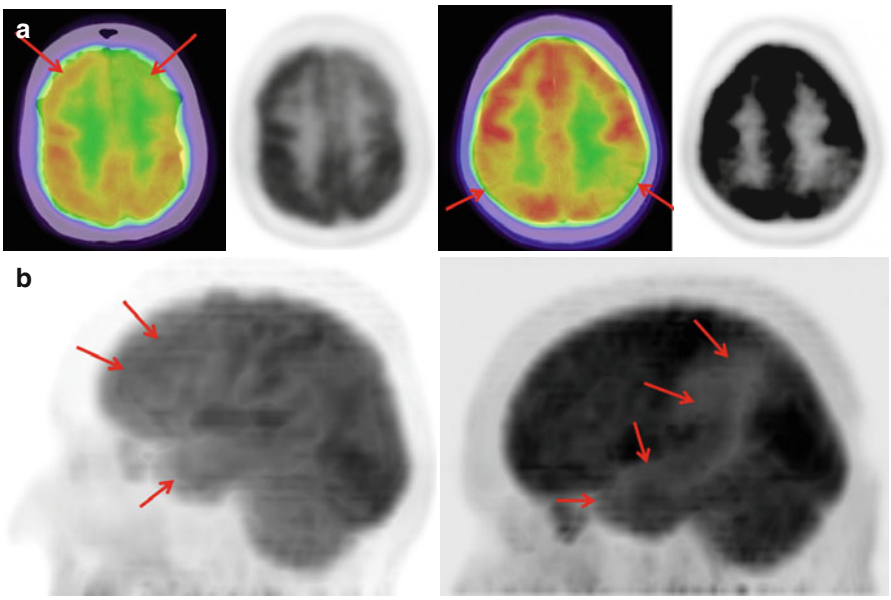

Fig. 14.7 Axial and MIP slice (**a**) and sagittal slice (**b**) from patient with dementia (Alzheimer's disease) showing hypometabolism (*arrows*) in the parietal and temporal region by sparing the motor cortex

radiopharmaceutical is minimal. HMPAO SPECT may demonstrate multiple patchy perfusion defects or reduced perfusion in one or more arterial territories. Amyloid imaging with ^{18}F-labeled radiotracers has recently been introduced for diagnosis of dementia, which is under further evaluations for clinical use. [J Nucl Med. 2011 Aug;52(8):1210-7. doi: 10.2967/jnumed.111.089730. Villemagne at al. Amyloid imaging with (18)F-florbetaben in Alzheimer disease and other dementias]

Epilepsy

In medically refractory epilepsy, surgery is contemplated to be of potential benefit to the patient. SPECT is used in cases where discrepancies arise between EEG finding and MRI.

During an episode of seizure, the metabolic activity of abnormally firing cells increases several fold which is associated with an increase in local blood flow. The radiopharmaceutical HMPAO can be injected during an ictal episode which reaches a steady state. The radiotracer remains bounded for about 6 h post-injection and can be imaged using rCBF SPECT demonstrating the epileptogenic focus [92]. Ictal SPECT shows good sensitivities in the correct lateralization of an electroencephalogram-defined epileptic focus in lesional and, to a lesser extent, non-lesional epilepsy.

Positron emission tomography (PET) using ^{18}F-FDG or ^{11}C-flumazenil will give a good detection rate of the epileptogenic zone in non-lesional cases and extratemporal epilepsy [93].

Nuclear Imaging in Cardiovascular System

Nuclear medicine imaging in the cardiovascular studies include gated/nongated myocardial perfusion imaging, myocardial viability studies, infarction imaging, ventricular function studies, and detection and quantitation of intracardiac shunts.

Exercise on a treadmill, or simulation of exercise by infusion of dipyridamole/adenosine/dobutamine, is used in conjunction with perfusion agents to increase radionuclide delivery to the normal myocardium. Stepwise increases in physical exercise are monitored by sequential electrocardiogram (ECG) and blood pressure and pulse measurements while the patient is queried for symptoms of angina. The radiopharmaceuticals widely used in myocardial perfusion scan are thallium-201 (Tl-201), Tc-99m sestamibi, and Tc-99m tetrofosmin. We will discuss the various aspects of myocardial perfusion imaging (MPI) with focus on Tl-201 imaging.

Radiopharmaceuticals

Thallium-201 is an analog of the potassium ion (K^+), which is delivered to capillary beds by regional blood flow and actively pumped into viable cells by the sodium/potassium (Na^+/K^+) adenosine triphosphatase pump. The effective half-life or 50 % washout of Tl-201 from the normal myocardium is about 4 h.

On the other hand, Tc-99m sestamibi is taken up by the perfused myocardium by passive diffusion and is bound in the myocyte, mostly within myocardial mitochondria. Tc-99m tetrofosmin is rapidly extracted from the blood by perfused myocardium in a fashion that resembles Tc-99m sestamibi. The two agents have proven to act clinically in a very similar manner, but availability and pricing make important considerations.

Clinical Application

Myocardial perfusion imaging demonstrates relative regional perfusion. Areas of myocardium with poor blood supply, usually because of atherosclerosis, fail to increase radiotracer uptake during the stress component. The most important feature of the myocardial perfusion test is comparison of the stress and rest images to detect areas of ischemia that are inadequately perfused at exercise yet still viable. These areas are redundantly called *reversibly ischemic*. A frequent location of ischemic tissue is immediately adjacent to an area of infarct. This is called *peri-infarct ischemia* and does not portend the same clinical significance as an ischemic or reversible zone. Abnormal anatomy in a coronary artery may not produce hemodynamically significant changes in blood flow to the myocardium, and not all ischemia is produced by large vessel atherosclerosis. Capillary disease in diabetics, left bundle branch block, vasospasm, vasculitis, or cardiomyopathy (dilated or hypertrophic) may produce ischemic myocardium even with normal arteries. Ischemia may

not be detected if there is inadequate exercise, inadequate pharmacologic challenge, or compensated triple-vessel disease. The myocardial perfusion scan also detects ischemia due to other causes (including left bundle branch block, coronary vasculitis, and small vessel disease) that cannot be seen on coronary arteriography and thereby reduces its apparent specificity.

Myocardial infarction produces layers of nonperfused scar tissue which are detected as areas of thin myocardium with decreased radiotracer uptake at both stress and rest imaging. The extent of an infarct, from subendocardial to transmural, is reflected by the size and degree of this perfusion defect. A single myocardial perfusion scan cannot determine the age of an infarct. Acute infarcts usually appear larger than old infarcts when imaged with Tl-201. Temporarily damaged cells around infarcted cells, referred to as stunned myocardium, will be hypokinetic/akinetic and will not hold on to the Tl-201 until recovered several weeks later.

PET is more expensive than standard myocardial perfusion imaging but offers the advantages of coincidence imaging, higher-energy photons, efficient attenuation correction, and different radiopharmaceuticals. PET agents can also be imaged on hybrid SPECT cameras or SPECT cameras with heavy collimators. PET scanning with coincidence detection allows high photon flux because collimators are not required. PET scans have higher-resolution images and fewer attenuation artifacts than standard MPI. Thus, PET scans may be the gold standard for MPI. PET perfusion is usually evaluated with rubidium-82 or ammonia-13 ($^{13}NH_3$), comparing the rest imaging with stress imaging, as in standard MPI. Other PET agents that are infrequently used for myocardial perfusion is ^{15}O water (^{15}O-H_2O). Viability of hibernating myocardium is evaluated with resting injection of fluorine-18 fluorodeoxyglucose (FDG). Myocardial oxygen consumption is often measured by ^{11}C-labeled acetate in conjunction with perfusion study [94–96]. Fatty acids undergo oxidation to yield energy for cardiac muscle, and its metabolism could be measured using ^{11}C-labeled palmitate radioligand.

Nuclear Imaging in Genitourinary System

The kidneys receive approximately 25 % of cardiac output and are one of the highly perfused organs. Though the widespread application and technical advancement of CT and MRI has reduced the use of nuclear medicine in assessing renal pathology, nuclear medicine is the choice for functional assessment and still is the gold standard for upper urinary tract obstruction and pyelonephritic scarring secondary to UTI.

The indications for diagnostic imaging usually depend upon the clinical presentation and the age of the patient. Frequently more than one imaging technique is required to fully evaluate the anatomy and physiology of the genitourinary tract.

The ^{99m}Tc-diethylenetriaminepenta-acetic acid (DTPA) and ^{51}Cr-ethylene diamine tetra-acetic acid (EDTA) are loosely bound to plasma protein and hence are freely filtered in the glomerulus. They are not reabsorbed from renal tubules back into the efferent vessels; the glomerular filtration represents its plasma clearance.

Hence, these can be used in the physiological study of glomerular filtration rate (GFR). Another radiopharmaceutical ^{99m}Tc 2, 3-dimercaptosuccinic acid (DMSA) is used for static and SPECT imaging of the kidneys.

Tubular transport tracers include technetium [^{99m}Tc], mercapto-acetyl-triglycine (MAG-3), and ^{99m}Tc dimercapto-succinic acid (DMSA); these agents identify renal cortical tissue and can localize ectopic renal tissue. The DMSA scan is the most accurate imaging modality for the diagnosis of acute pyelonephritis, the decreased accumulation of the tracer in the renal parenchyma is secondary to inflammatory edema, the resultant decreased blood flow and cellular enzymatic activity [97].

^{99m}Tc DTPA is used in diuretic renography. It is mainly used in the differential diagnosis of hydronephrosis/hydroureteronephrosis as the cause for obstructive nephropathy. To distinguish the conditions causing obstructive nephropathy is pertinent as medical management is usually indicated for a dilated/nonobstructed urinary tract, while surgery is recommended for a dilated/obstructed tract to improve the renal function [98].

Nuclear Imaging in Infection and Inflammation

Scintigraphic evaluation of infection and inflammation is a very broad topic in itself and beyond the scope of this chapter; we will briefly elaborate the numerous radiopharmaceuticals and imaging techniques like gallium-67 (Ga-67) citrate, radiolabeled leukocytes (WBC), and Tc-99m-fanolesomab imaging in evaluation of inflammation and infection.

Gallium-67

Gallium-67 has a half-life of 78.1 h, with principal photon energies of 93, 184, and 296 keV; it's been used for imaging over the last three decades, but a poor photon yield per disintegration makes it a suboptimal imaging agent [99].

About 90 % of circulating Ga-67 is in the plasma, nearly all transferrin bound. Increased vascularity and/or increased vascular membrane permeability result in increased delivery and accumulation of transferrin-bound Ga-67 at inflammatory foci. Ga-67 also binds to lactoferrin, which is present in high concentrations in inflammatory foci. Direct bacterial uptake may also account for some Ga-67 accumulation in infection. Siderophores, low-molecular-weight chelates produced by bacteria, have a high affinity for Ga-67. The siderophore-Ga-67 complex is presumably transported into the bacterium, where it eventually is phagocytosed by macrophages. Although some Ga-67 may be transported bound to leukocytes, it is important to note that, even in the absence of circulating leukocytes, Ga-67 accumulates in infection [99]. Imaging is usually performed 18–72 h after injection of Ga-67.

Various indications for Ga-67 imaging are as follows:

1. Ga-67 imaging is the radionuclide procedure of choice in the detection of infections unique to the immunocompromised patients.
2. Ga-67 is extremely sensitive to detection of pulmonary inflammations: sarcoidosis, interstitial pneumonitis, drug reactions, collagen vascular disease, and pneumoconioses.
3. Interstitial nephritis: Ga-67 can be helpful in differentiating interstitial nephritis from acute tubular necrosis in the acute setting.
4. Fever of undetermined origin (FUO) is an illness of at least 3 weeks duration with several episodes of fever exceeding 38.3 °C and no confirmed diagnosis. Ga-67 is typically reserved for those situations in which other imaging tests fail to localize the source of the fever. Since Ga-67 accumulates in foci of infection, inflammation, and tumor, it is often preferred over WBC imaging for this indication [99, 100].
5. Spinal osteomyelitis: Ga-67 imaging is frequently performed in conjunction with bone scintigraphy [101].

Radiolabeled Leukocytes

The only approved methods in radiolabeled leukocytes technique are the lipophilic compounds indium-111 (In-111) oxyquinoline and ^{99m}Tc-HMPAO (hexamethyl propyleneamine oxime). Advantages of the In-111 label are its stability and a virtually constant normal distribution of activity limited to the liver, spleen, and bone marrow. The 67-h physical half-life of In-111 permits delayed imaging, which is particularly valuable for musculoskeletal infection. Disadvantages of the In label include a low photon flux, less-than-ideal photon energies, and the fact that a 24-h interval between injection and imaging is generally required [100].

Advantages of Tc-99m-WBCs include a photon energy that is optimal for imaging using current instrumentation, a high photon flux, and the ability to detect abnormalities within a few hours after injection. The instability of the label and the 6-h half-life of Tc-99m are disadvantages when delayed 24-h imaging is needed. This occurs in those infections that tend to be indolent in nature and for which several hours may be necessary for accumulation of a sufficient quantity of labeled leukocytes to be successfully imaged [100].

Clinical Utility

Using Tc-99m-WBCs, diffuse pulmonary uptake on images obtained more than 4 h after injection of labeled cells is associated with opportunistic infection, radiation pneumonitis, pulmonary drug toxicity and ARDS. This pattern is almost never seen, however, in bacterial pneumonia [102]. Diffuse pulmonary uptake of WBCs is also seen in septic patients with normal chest radiographs and who have no clinical evidence of respiratory tract inflammation or infection.

^{111}In-WBCs do not accumulate in normal bowel. Such activity is always abnormal and is seen in antibiotic-associated or pseudomembranous colitis, infectious colitis, inflammatory bowel disease, ischemic colitis, and GI bleeding [100, 103]. Also radiolabeled WBCs do not accumulate in normally healing surgical wounds, so the presence of such activity indicates infection although there are certain exceptions.

Both Ga-67 and WBC imaging are confirmatory in detecting myocardial abscesses in patients with infective endocarditis [100]. WBC imaging is the radionuclide procedure of choice for diagnosing prosthetic vascular graft infection, with a sensitivity of more than 90 % [100].

WBC imaging is very sensitive for detecting inflammatory bowel disease and can be used as a screening test to determine which patients need to undergo more invasive investigation.

Tc-99m Fanolesomab

Tc-99m fanolesomab, a monoclonal murine M-class immunoglobulin, binds to CD15 receptors present on leukocytes. This agent presumably binds to circulating neutrophils that eventually migrate to the focus of infection, as well as to neutrophils or neutrophil debris containing CD15 receptors, already sequestered in the area of infection. At present, Tc-99m fanolesomab is approved for only diagnosis of equivocal appendicitis in patients older than 5 years.

Pediatric Nuclear Medicine

The nuclear scanning of children is not entirely equivalent in adults. The growth process and radiopharmaceutical distribution are different in children. Moreover, high-resolution images are necessary because an organ in a child may be just one fourth the size of an adult's yet have the same number of receptors attaching to the radiopharmaceutical. Children also suffer from different types of cancers with different disease patterns and are more likely to have more aggressive tumors. For this reason, most nuclear physicians have replaced localized bone scanning with whole-body images in children [104].

Nuclear medicine is only conservatively used in pediatric cases. It is used in detection of primary and secondary malignancies, pyrexia of unknown origin (PUO), cause of urinary retention, bone tumors, infection, trauma, GI bleeding, etc. ^{99m}Tc phosphate is the common tracer used for bone scans. FDG-PET is used in some common pediatric malignancies like brain neoplasms and lymphomas and in certain less common malignancies like neuroblastoma (even in cases that are not metaiodobenzylguanidine (MIBG) avid detected by SPECT), bone and soft tissue sarcoma, Wilm's tumor, and hepatoblastoma [105].

Future Trends and Outlook

Nuclear medicine is one of the fastest growing fields of medical science. The current progress in nuclear medicine is creating fresh directions in imaging of the body at the molecular level providing greater information about the cellular pathology, injurious signal, and its downstream pathway in the process of cell death including apoptosis and defects in metabolic pathways. Insight into the molecular nature of cancer and other disease processes provides a new dimension of target-oriented therapeutic options. Molecular imaging will leverage the future clinical trials involving molecular therapies. It may provide guidance for several treatment strategies that are targeted at the molecular level such as immune guided therapy, hormonal therapy, cancer chemotherapy, and gene therapy. In order to take nuclear medicine to that level, a synchronous advancement in synthetic chemistry, signal acquisition, and data processing technique and hardware are the prerequisites.

Currently, biopsy is considered the gold standard for establishing the diagnosis of several diseases, but biopsy findings are based on samples collected from small portion of a tumor at a single point in space and time. But the targets are known to change dynamically over time and space. Hence, biopsy-based clinical practice may not address the exact in vivo molecular abnormality that leads to the disease or tumor. Molecular imaging technology is seen as a promising tool in bridging this gap in knowledge.

Advancement in synthetic chemistry with newer radiopharmaceutical tracers having high specificity for the receptors or antigens in the diseased or malignant tissues is required for target identification for molecular therapies, tumor profiling, therapeutic selection, monitoring of early treatment response and monitoring of disease recurrence. In fact, the future trend of molecular medicine will be towards this direction extending far beyond what the currently available tracers are capable of. Most of the contemporary agents rely on processes that are fairly generic to malignant transformation and not necessarily specific to any particular cancer [10]. For instance, ^{18}F-FDG is taken up by almost all cells of the body that utilize glucose making it highly nonspecific but with high sensitivity. Newer agents like fluoroestradiol (FES) and fluorodihydroxytestosterone (FDHT) are specific ligands for estrogen receptor (ER) and androgen receptor (AR), respectively. FES is used to image the ER + breast carcinoma that influence the treatment modality as 30–77 % of ER + patients show a favorable response to hormonal therapy at far less morbidity than alternative chemotherapy [106]. An array of radiopharmaceutical tracers targeting various mechanisms specific for malignancy and diseases is being evaluated continuously, a discussion on which is beyond the scope of this book.

Molecular imaging provides an effective monitoring and early feedback of therapeutic effect on the tumor tissue. The early molecular response to therapy which could be identified by PET within weeks could influence the treatment plan, should the therapeutic agent used fails, which could be replaced with a more effective therapeutic agent. Conventional imaging may take months to provide feedback on therapeutic response based on morphologic information and may even lead to selection of cells resistant to chemotherapy. Several targeted therapy with specific ligands tagged with

radionuclide could be monitored for its therapeutic efficiency. Molecular imaging serves as a promising modality in monitoring the treatment efficacy and follow-up.

The hybrid PET/CT complimenting each other's deficiency offers excellent information about the function with good spatial and temporal resolution. But MRI provides greater soft tissue contrast and is the modality of choice for soft tissue imaging. Hybrid PET/MR was thus conceptualized but is currently not in routine clinical practice.

The combination of PET functional imaging and MRI structural imaging with excellent soft tissue contrast is the most yearned modality that is awaited to be added in the patient care diagnostic imaging chain. The PET/MR system might offer simultaneous information on anatomy, functionality, and biochemistry of the tissues and cells.

The scenario is optimistic and, PET/MR hybrid technology has the potential to become the imaging modality of choice for neurological studies, vast range of oncology studies, and may also have a great role in stem cell therapy. With this elaborate discussion on various aspects of nuclear medicine, we conclude that optimal diagnosis using radionuclides requires careful consideration of the patient, indications for the study, and the imaging modalities. Nuclear medicine imaging techniques and radionuclide imaging plays a pivotal role in the diagnosis of typical systemic diseases and will continue to do so in future, but still more research work is required to achieve its place in medical practice.

References

1. Brownell GL, Burnham CA, Chesler DA. Lateral and transverse section imaging with the MGH positron camera. Prog Nucl Med. 1978;4:158–64.
2. Phelps ME, Hoffman EJ, Mullani NA, Ter-Pogossian MM. Application of annihilation coincidence detection to transaxial reconstruction tomography. J Nucl Med. 1975;16:210–24.
3. Giesel FL, Mehndiratta A, Locklin J, McAuliffe MJ, White S, Choyke PL, Knopp MV, Wood BJ, Haberkorn U, von Tengg-Kobligk H. Image fusion using CT, MRI and PET for treatment planning, navigation and follow up in percutaneous RFA. Exp Oncol. 2009;31(2):106–14.
4. Gambhir SS, Czernin J, Schwimmer J, Silverman DH, Coleman RE, Phelps ME. A tabulated summary of the FDG PET literature. J Nucl Med. 2001;42:1S–93.
5. Gallagher BM, Ansari A, Atkins H, et al. Radiopharmaceuticals XXVII. 18F-labeled 2-deoxy-2-fluoro-d-glucose as a radiopharmaceutical for measuring regional myocardial glucose metabolism in vivo: tissue distribution and imaging studies in animals. J Nucl Med. 1977; 18:990–6.
6. Reivich M, Kuhl D, Wolf A, et al. The [18F] fluorodeoxyglucose method for the measurement of local cerebral glucose utilization in man. Circ Res. 1979;44:127–37.
7. Czernin J, Phelps ME. Positron emission tomography scanning: current and future applications. Ann Rev Med. 2002;53:89–112.
8. DeGrado TR, Baldwin SW, Wang S, et al. Synthesis and evaluation of (18)F-labeled choline analogs as oncologic PET tracers. J Nucl Med. 2001;42:1805–14.
9. Bruehlmeier M, Roelcke U, Schubiger PA, Ametamey SM. Assessment of hypoxia and perfusion in human brain tumors using PET with 18F-fluoromisonidazole and 15O-H2O. J Nucl Med. 2004;45:1851–9.

10. Hicks RJ. Beyond FDG: novel PET tracers for cancer imaging. Cancer Imaging. 2004; 4:22–4.
11. Otte A, Dierckx RA. Good clinical practice: a plea for nuclear medicine. Nucl Med Commun. 2005;26:561.
12. Otte A, Maier-Lenz H, Dierckx RA. Good clinical practice: historical background and key aspects. Nucl Med Commun. 2005;26:563–74.
13. De Vos FJ, De DM, Dierckx RA. The good laboratory practice and good clinical practice requirements for the production of radiopharmaceuticals in clinical research. Nucl Med Commun. 2005;26:575–9.
14. Zanzonico P. Routine quality control of clinical nuclear medicine instrumentation: a brief review. J Nucl Med. 2008;49:1114–31.
15. Strauss LG, Conti PS. The applications of PET in clinical oncology. J Nucl Med. 1991; 32:623–48.
16. Bar-Shalom R, Valdivia AY, Blaufox MD. PET imaging in oncology. Semin Nucl Med. 2000;30:150–85.
17. Tochon-Danguy HJ, Sachinidis JI, Egan GF, et al. Positron emission tomography: radioisotope and radiopharmaceutical production. Australas Phys Eng Sci Med. 1999;22:136–44.
18. Scott AM. Current status of positron emission tomography in oncology. Australas Radiol. 2002;46:154–62.
19. Hicks RJ, Binns DS, Fawcett ME, et al. Positron emission tomography (PET): experience with a large-field-of-view three-dimensional PET scanner. Med J Aust. 1999;171:529–32.
20. Som P, Atkins HL, Bandoypadhyay D, et al. A fluorinated glucose analog, 2-fluoro-2-deoxy-D-glucose (F-18): nontoxic tracer for rapid tumor detection. J Nucl Med. 1980;21:670–5.
21. Reutens DC, Bittar RG, Tochon-Danguy H, Scott AM. Clinical applications of [(15)O] H(2) O PET activation studies. Clin Positron Imaging. 1999;2:145–52.
22. Scott AM, Larson SM. Tumor imaging and therapy. Radiol Clin North Am. 1993;31: 859–79.
23. Conti PS, Lilien DL, Hawley K, Keppler J, Grafton ST, Bading JR. PET and [18F]-FDG in oncology: a clinical update. Nucl Med Biol. 1996;23:717–35.
24. Valk PE. Randomized controlled trials are not appropriate for imaging technology evaluation. J Nucl Med. 2000;41:1125–6.
25. Berlangieri SU, Scott AM, Knight SR, et al. F-18 fluorodeoxyglucose positron emission tomography in the non-invasive staging of non-small cell lung cancer. Eur J Cardiothorac Surg. 1999;16 Suppl 1:S25–30.
26. Findlay M, Young H, Cunningham D, et al. Noninvasive monitoring of tumor metabolism using fluorodeoxyglucose and positron emission tomography in colorectal cancer liver metastases: correlation with tumor response to fluorouracil. J Clin Oncol. 1996;14:700–8.
27. Damian DL, Fulham MJ, Thompson E, Thompson JF. Positron emission tomography in the detection and management of metastatic melanoma. Melanoma Res. 1996;6:325–9.
28. Kiffer JD, Berlangieri SU, Scott AM, et al. The contribution of 18F-fluoro-2-deoxy-glucose positron emission tomographic imaging to radiotherapy planning in lung cancer. Lung Cancer. 1998;19:167–77.
29. Shon IH, O'doherty MJ, Maisey MN. Positron emission tomography in lung cancer. Semin Nucl Med. 2002;32:240–71.
30. Berlangieri SU, Scott AM. Metabolic staging of lung cancer. N Engl J Med. 2000;343:290–2.
31. Di CG, Brooks RA. PET-FDG of untreated and treated cerebral gliomas. J Nucl Med. 1988; 29:421–3.
32. Jeong HJ, Chung JK, Kim YK, et al. Usefulness of whole-body (18) F-FDG PET in patients with suspected metastatic brain tumors. J Nucl Med. 2002;43:1432–7.
33. Weber WA, Wester HJ, Grosu AL, et al. O-(2-[18F] fluoroethyl)-L-tyrosine and L-[methyl-11C] methionine uptake in brain tumors: initial results of a comparative study. Eur J Nucl Med. 2000;27:542–9.
34. Gupta N, Bradfield H. Role of positron emission tomography scanning in evaluating gastrointestinal neoplasms. Semin Nucl Med. 1996;26:65–73.

35. Lowe VJ, Fletcher JW, Gobar L, et al. Prospective investigation of positron emission tomography in lung nodules. J Clin Oncol. 1998;16:1075–84.
36. Kratochwil C, Haberkorn U, Giesel FL. PET/CT for diagnostics and therapy stratification of lung cancer. Radiologe. 2010;50(8):684–91. doi:10.1007/s00117-009-1960-6. Review. German.
37. Gould MK, Maclean CC, Kuschner WG, Rydzak CE, Owens DK. Accuracy of positron emission tomography for diagnosis of pulmonary nodules and mass lesions: a meta-analysis. JAMA. 2001;285:914–24.
38. Vansteenkiste JF, Stroobants SG, De Leyn PR, et al. Mediastinal lymph node staging with FDG-PET scan in patients with potentially operable non-small cell lung cancer: a prospective analysis of 50 cases. Leuven Lung Cancer Group. Chest. 1997;112:1480–6.
39. Valk PE, Pounds TR, Hopkins DM, et al. Staging non-small cell lung cancer by whole-body positron emission tomographic imaging. Ann Thorac Surg. 1995;60:1573–81.
40. Bury T, Dowlati A, Paulus P, et al. Whole-body 18FDG positron emission tomography in the staging of non-small cell lung cancer. Eur Respir J. 1997;10:2529–34.
41. Gambhir SS, Hoh CK, Phelps ME, Madar I, Maddahi J. Decision tree sensitivity analysis for cost-effectiveness of FDG-PET in the staging and management of non-small-cell lung carcinoma. J Nucl Med. 1996;37:1428–36.
42. Giesel F, Stefanova M, Schwartz LH, Afshar-Oromieh A, Eisenhut M, Haberkorn U, Kratochwil C. Impact of peptide receptor radionuclide therapy on the 68Ga-DOTATOC-PET/CT uptake in normal tissue. Q J Nucl Med Mol Imaging. 2013;57(2):171–6.
43. Giesel FL, Kratochwil C, Mehndiratta A, Wulfert S, Moltz JH, Zechmann CM, Kauczor HU, Haberkorn U, Ley S. Comparison of neuroendocrine tumor detection and characterization using DOTATOC-PET in correlation with contrast enhanced CT and delayed contrast enhanced MRI. Eur J Radiol. 2012;81(10):2820–5.
44. Yasuda S, Fujii H, Nakahara T, et al. 18F-FDG PET detection of colonic adenomas. J Nucl Med. 2001;42:989–92.
45. Arulampalam TH, Costa DC, Bomanji JB, Ell PJ. The clinical application of positron emission tomography to colorectal cancer management. Q J Nucl Med. 2001;45:215–30.
46. Schiepers C, Penninckx F, De VN, et al. Contribution of PET in the diagnosis of recurrent colorectal cancer: comparison with conventional imaging. Eur J Surg Oncol. 1995;21:517–22.
47. Heriot AG, Hicks RJ, Drummond EG, et al. Does positron emission tomography change management in primary rectal cancer? A prospective assessment. Dis Colon Rectum. 2004;47:451–8.
48. Naumann R, Beuthien-Baumann B, Reiss A, et al. Substantial impact of FDG PET imaging on the therapy decision in patients with early-stage Hodgkin's lymphoma. Br J Cancer. 2004;90:620–5.
49. Delbeke D, Martin WH, Morgan DS, et al. 2-Deoxy-2-[F-18]fluoro-D-glucose imaging with positron emission tomography for initial staging of Hodgkin's disease and lymphoma. Mol Imaging Biol. 2002;4:105–14.
50. Jerusalem G, Beguin Y, Najjar F, et al. Positron emission tomography (PET) with 18F-fluorodeoxyglucose (18F-FDG) for the staging of low-grade non-Hodgkin's lymphoma (NHL). Ann Oncol. 2001;12:825–30.
51. Schoder H, Meta J, Yap C, et al. Effect of whole-body (18) F-FDG PET imaging on clinical staging and management of patients with malignant lymphoma. J Nucl Med. 2001;42:1139–43.
52. Foo SS, Mitchell PL, Berlangieri SU, Smith CL, Scott AM. Positron emission tomography scanning in the assessment of patients with lymphoma. Intern Med J. 2004;34:388–97.
53. Spaepen K, Stroobants S, Dupont P, et al. Prognostic value of positron emission tomography (PET) with fluorine-18 fluorodeoxyglucose ([18F] FDG) after first-line chemotherapy in non-Hodgkin's lymphoma: is [18F] FDG-PET a valid alternative to conventional diagnostic methods? J Clin Oncol. 2001;19:414–9.
54. Mikhaeel NG, Timothy AR, Hain SF, O'doherty MJ. 18-FDG-PET for the assessment of residual masses on CT following treatment of lymphomas. Ann Oncol. 2000;11 Suppl 1:147–50.
55. Balch CM, Soong SJ, Gershenwald JE, et al. Prognostic factors analysis of 17,600 melanoma patients: validation of the American Joint Committee on Cancer melanoma staging system. J Clin Oncol. 2001;19:3622–34.

56. Mijnhout GS, Hoekstra OS, van Tulder MW, Teule GJ, Deville WL. Systematic review of the diagnostic accuracy of (18) F-fluorodeoxyglucose positron emission tomography in melanoma patients. Cancer. 2001;91:1530–42.
57. Schwimmer J, Essner R, Patel A, et al. A review of the literature for whole-body FDG PET in the management of patients with melanoma. Q J Nucl Med. 2000;44:153–67.
58. Adams S, Baum RP, Stuckensen T, Bitter K, Hor G. Prospective comparison of 18F-FDG PET with conventional imaging modalities (CT, MRI, US) in lymph node staging of head and neck cancer. Eur J Nucl Med. 1998;25:1255–60.
59. Hannah A, Scott AM, Tochon-Danguy H, et al. Evaluation of 18 F-fluorodeoxyglucose positron emission tomography and computed tomography with histopathologic correlation in the initial staging of head and neck cancer. Ann Surg. 2002;236:208–17.
60. Paulus P, Sambon A, Vivegnis D, et al. 18FDG-PET for the assessment of primary head and neck tumors: clinical, computed tomography, and histopathological correlation in 38 patients. Laryngoscope. 1998;108:1578–83.
61. Keyes Jr JW, Watson Jr NE, Williams III DW, Greven KM, McGuirt WF. FDG PET in head and neck cancer. AJR Am J Roentgenol. 1997;169:1663–9.
62. Greven KM, Keyes Jr JW, Williams III DW, McGuirt WF, Joyce III WT. Occult primary tumors of the head and neck: lack of benefit from positron emission tomography imaging with 2-[F-18]fluoro-2-deoxy-D-glucose. Cancer. 1999;86:114–8.
63. Farber LA, Benard F, Machtay M, et al. Detection of recurrent head and neck squamous cell carcinomas after radiation therapy with 2-18F-fluoro-2-deoxy-D-glucose positron emission tomography. Laryngoscope. 1999;109:970–5.
64. Rege S, Safa AA, Chaiken L, Hoh C, Juillard G, Withers HR. Positron emission tomography: an independent indicator of radiocurability in head and neck carcinomas. Am J Clin Oncol. 2000;23:164–9.
65. Wahl RL, Siegel BA, Coleman RE, Gatsonis CG. Prospective multicenter study of axillary nodal staging by positron emission tomography in breast cancer: a report of the staging breast cancer with PET Study Group. J Clin Oncol. 2004;22:277–85.
66. Moon DH, Maddahi J, Silverman DH, Glaspy JA, Phelps ME, Hoh CK. Accuracy of whole-body fluorine-18-FDG PET for the detection of recurrent or metastatic breast carcinoma. J Nucl Med. 1998;39:431–5.
67. Bender H, Kirst J, Palmedo H, et al. Value of 18fluoro-deoxyglucose positron emission tomography in the staging of recurrent breast carcinoma. Anticancer Res. 1997;17: 1687–92.
68. Luketich JD, Friedman DM, Weigel TL, et al. Evaluation of distant metastases in esophageal cancer: 100 consecutive positron emission tomography scans. Ann Thorac Surg. 1999;68: 1133–6.
69. Meltzer CC, Luketich JD, Friedman D, et al. Whole-body FDG positron emission tomographic imaging for staging esophageal cancer comparison with computed tomography. Clin Nucl Med. 2000;25:882–7.
70. Lerut T, Flamen P. Role of FDG-PET scan in staging of cancer of the esophagus and gastroesophageal junction. Minerva Chir. 2002;57:837–45.
71. Fukunaga T, Okazumi S, Koide Y, Isono K, Imazeki K. Evaluation of esophageal cancers using fluorine-18-fluorodeoxyglucose PET. J Nucl Med. 1998;39:1002–7.
72. Einhorn N, Nilsson B, Sjovall K. Factors influencing survival in carcinoma of the ovary. Study from a well-defined Swedish population. Cancer. 1985;55:2019–25.
73. Karlan BY, Hawkins R, Hoh C, et al. Whole-body positron emission tomography with 2-[18F]-fluoro-2-deoxy-D-glucose can detect recurrent ovarian carcinoma. Gynecol Oncol. 1993;51:175–81.
74. Hubner KF, McDonald TW, Niethammer JG, Smith GT, Gould HR, Buonocore E. Assessment of primary and metastatic ovarian cancer by positron emission tomography (PET) using 2-[18F]deoxyglucose (2-[18F]FDG). Gynecol Oncol. 1993;51:197–204.
75. Stephens AW, Gonin R, Hutchins GD, Einhorn LH. Positron emission tomography evaluation of residual radiographic abnormalities in postchemotherapy germ cell tumor patients. J Clin Oncol. 1996;14:1637–41.

76. Yeh S, Imbriaco M, Larson S, Garza D, Zhang JJ, Kalaigian H, Finn RD, Reddy D, Horowitz SM, Goldsmith SJ, Scher HI. Detection of bony metastases of androgen independent prostate cancer by FDG–PET. Nucl Med Biol. 1996;23:693–7.
77. Shreve PD, Grossmann HB, Gross MD, Wahl RL. Metastatic prostate cancer: initial findings of PET with 2-deoxy-2-[F-18]-fluoro-D-glucose. Radiology. 1996;199:751–6.
78. Shvarts O, Han KR, Seltzer M, Pantuck AJ, Belldegrun AS. Positron emission tomography in urologic oncology. Cancer Control. 2002;9:335–42.
79. Effert PJ, Bares R, Handt S, Wolff JM, Bull D, Jakes G. Metabolic imaging of untreated prostate cancer by positron emission tomography with 18-fluorine-labeled deoxyglucose. J Urol. 1996;155:994–8.
80. Hara T. ^{18}F–fluorocholine: a new oncologic PET tracer. J Nucl Med. 2001;42:1815–6.
81. DeGrado TR, Coleman RE, Wang S, Baldwin SW, Orr MD, Robertson CN, Polascik TJ, Price DT. Synthesis and evaluation of ^{18}F–labeled choline as an oncologic tracer for positron emission tomography: initial findings in prostate cancer. Cancer Res. 2000;61:110–7.
82. Beheshti M, Imamovic L, Broinger G, Vali R, Waldenberger P, Stoiber F, Nader M, Gruy B, Janetschek G, Langsteger W. ^{18}F choline PET/CT in the preoperative staging of prostate cancer in patients with intermediate or high risk of extracapsular disease: a prospective study of 130 patients. Radiology. 2010;254:925–33.
83. Oyama N, Miller TR, Dehdashti F, Siegel BA, Fischer KC, Michalski JM, Kibel AS, Andriole GL, Picus J, Welch MJ. ^{11}C–acetate PET imaging of prostate cancer: detection of recurrent disease at PSA relapse. J Nucl Med. 2003;44:549–55.
84. Kato T, Tsukamoto E, Kuge Y, Takei T, Shiga T, Shinohara N, Katoh C, Nakada K, Tamaki N. Accumulation of [^{11}C]acetate in normal prostate and benign prostatic hyperplasia: comparison with prostate cancer. Eur J Nucl Med. 2002;29:1492–5.
85. Afshar-Oromieh A, Haberkorn U, Eder M, Eisenhut M, Zechmann CM. [68Ga]Gallium-labelled PSMA ligand as superior PET tracer for the diagnosis of prostate cancer: comparison with 18F-FECH. Eur J Nucl Med Mol Imaging. 2012;39(6):1085–6.
86. Nunez R, Macapinlac HA, Yeung HWD, Akhurst T, Cai S, Osman I, Gonen M, Riedel E, Scher HI, Larson SM. Combined ^{18}F–FDG and ^{11}C–methionine PET scans in patients with newly progressive metastatic prostate cancer. J Nucl Med. 2002;43:46–55.
87. Hoffman JM, Welsh-Bohmer KA, Hanson M, et al. FDG PET imaging in patients with pathologically verified dementia. J Nucl Med. 2000;41:1920–8.
88. Andersson JD, Varnas K, Cselenyi Z, et al. Radiosynthesis of the candidate beta-amyloid radioligand [(11)C]AZD2184: positron emission tomography examination and metabolite analysis in cynomolgus monkeys. Synapse. 2010;64:733–41.
89. O'Brien JT, Eagger S, Syed GM, Sahakian BJ, Levy R. A study of regional cerebral blood flow and cognitive performance in Alzheimer's disease. J Neurol Neurosurg Psychiatry. 1992; 55:1182–7.
90. Jagust W, Thisted R, Devous Sr MD, et al. SPECT perfusion imaging in the diagnosis of Alzheimer's disease: a clinical-pathologic study. Neurology. 2001;56:950–6.
91. Schmidt D, Zimmermann R, Lewczuk P, et al. Confirmation rate of blinded (99m)Tc-SPECT compared to neurochemical dementia biomarkers in CSF in patients with Alzheimer disease. J Neural Transm. 2010;117(9):1111–4.
92. Devous Sr MD, Thisted RA, Morgan GF, Leroy RF, Rowe CC. SPECT brain imaging in epilepsy: a meta-analysis. J Nucl Med. 1998;39:285–93.
93. Asenbaum S, Baumgartner C. Nuclear medicine in the preoperative evaluation of epilepsy. Nucl Med Commun. 2001;22:835–40.
94. Wadsak W, Mitterhauser M. Basics and principles of radiopharmaceuticals for PET/CT. Eur J Radiol. 2010;73:461–9.
95. Tu Z, Mach RH. C-11 radiochemistry in cancer imaging applications. Curr Top Med Chem. 2010;10:1060–95.
96. Schlyer DJ. PET tracers and radiochemistry. Ann Acad Med Singapore. 2004;33:146–54.
97. Rushton HG, Majd M. Dimercaptosuccinic acid renal scintigraphy for the evaluation of pyelonephritis and scarring: a review of experimental and clinical studies. J Urol. 1992;148:1726–32.

98. Fommei E, Volterrani D. Renal nuclear medicine. Semin Nucl Med. 1995;25:183–94.
99. Palestro CJ. The current role of gallium imaging in infection. Semin Nucl Med. 1994;24: 128–41.
100. Love C, Palestro CJ. Radionuclide imaging of infection. J Nucl Med Technol. 2004;32: 47–57.
101. Palestro CJ, Torres MA. Radionuclide imaging in orthopedic infections. Semin Nucl Med. 1997;27:334–45.
102. Love C, Opoku-Agyemang P, Tomas MB, Pugliese PV, Bhargava KK, Palestro CJ. Pulmonary activity on labeled leukocyte images: physiologic, pathologic, and imaging correlation. Radiographics. 2002;22:1385–93.
103. Palestro CJ, Torres MA. Radionuclide imaging of nonosseous infection. Q J Nucl Med. 1999; 43:46–60.
104. Kotz D. Pediatric nuclear medicine: special issues, unique clinical studies. J Nucl Med. 1998; 39:13N–4, 26N.
105. Jadvar H, Connolly LP, Fahey FH, Shulkin BL. PET and PET/CT in pediatric oncology. Semin Nucl Med. 2007;37:316–31.
106. Schellingerhout D, Gelovani J. Clinical trials in a molecular world. Neuroimaging Clin N Am. 2006;16:681–94, ix.
107. Mettler FA, Huda W, Yoshizumi TT, Mahesh M. Effective doses in radiology and diagnostic nuclear medicine: a catalog. Radiology. 2008;248(1):254–63.
108. Wall BF, Hart D. Revised radiation doses for typical x-ray examinations. Br J Radiol. 1997; 70(833):437–9.